Electronic Supplementary Material (ESI) for Chemical Communications

Negative area compressibility in silver(I) tricyanomethanide

SUPPLEMENTARY INFORMATION

Sarah A. Hodgson,[1] Jasper Adamson,[1] Sarah J. Hunt,[1] Matthew J. Cliffe,[1] Andrew B. Cairns,[1] Amber L. Thompson,[1] Matthew G. Tucker,[2,3] Nicholas P. Funnell,[1] and Andrew L. Goodwin[1*]

[1]Department of Chemistry, University of Oxford, Inorganic Chemistry Laboratory, South Parks Road, Oxford OX1 3QR, U.K.

[2]ISIS Facility, Rutherford Appleton Laboratory, Chilton, Didcot, Oxfordshire OX11 0QX, U.K.

[3]Diamond Light Source, Harwell Campus, Didcot, Oxfordshire OX11 0DE, U.K.

[*]To whom correspondence should be addressed; E-mail: andrew.goodwin@chem.ox.ac.uk.

Submitted to Chemical Communications

Contents

1 Synthesis of Ag(*tcm*)

All reagents were obtained from commercial suppliers (Sigma Aldrich and Alfa Aesar) and used as delivered. Suitable precautions were taken when handling potassium tricyanomethanide, K(*tcm*); in particular, contact with strong acids was avoided in order to minimise all risk of evolving HCN.

Single-crystal samples were prepared as follows: saturated aqueous solutions of $AgNO_3$ (50 mg) and K(*tcm*) (50 mg) were added to opposite sides of a single glass H-cell. The cell was filled carefully with ice-cold H_2O. Over a period of 7 d, colourless transparent crystals of Ag(*tcm*) grew on the arms of the H-cell.

Powder samples were readily prepared by precipitation from equimolar saturated aqueous solutions of $AgNO_3$ and K(*tcm*), followed by filtering, washing (H_2O) and drying under vacuum (50 °C).

2 Experimental Methods: Crystallographic Measurements

2.1 Variable-Temperature Single-Crystal X-Ray Diffraction

Single-crystal X-ray diffraction measurements were performed using an Agilent Technologies SuperNova (Mo Kα radiation, λ = 0.71073 Å) fitted with an Oxford Cryosystems cryostream.[S1] A small crystal, with dimensions 0.044 mm × 0.052 mm × 0.094 mm, was mounted on a glass fibre using nail varnish. Full data collections were performed at temperature intervals of 10 K, on heating and subsequent cooling, between 100 and 250 K. Unit cell parameters were determined and refined using CrysAlisPro. The structure was solved with SIR92[S2] and refined by full-matrix least squares using CRYSTALS.[S3] All atoms were refined anisotropically against F^2. A thermal-similarity constraint was applied to the C1 and N1 atoms for all heating data and for cooling data collected between 210 and 250 K.

2.2 Variable-Pressure Single-Crystal X-ray Diffraction

Variable-pressure single-crystal X-ray diffraction measurements were performed using an Agilent Technologies Gemini diffractometer (Mo Kα radiation, λ = 0.71073 Å). A single crystal of Ag(*tcm*) was loaded in a Merrill-Bassett diamond anvil cell with an opening angle of 85°, equipped with a steel gasket and beryllium backing discs. A small ruby chip was also loaded in the cell allowing pressure determination *via* ruby fluorescence.[S4] Fluorinert was used as pressure-transmitting medium. Data were collected at four pressure points between ambient pressure and 2.39 GPa. CrysAlisPro was used to determine the unit cell and the strategy required for the data collection. The data were integrated with CrysAlisPro. Reflections arising from the Be backing discs and the diamond anvils were omitted. The crystal structure was solved using SIR92[S2] and refined against F^2 using CRYSTALS.[S3] All non-silver atoms were refined isotropically with geometric restraints owing to a poor data-to-parameter ratio owing to shading of reciprocal space by the diamond anvil cell body.

2.3 Variable-Pressure Neutron Powder Diffraction

High-pressure neutron powder diffraction measurements were performed on the PEARL instrument at the ISIS neutron spallation source using a V4 Paris-Edinburgh cell equipped with zirconia-toughened alumina anvils. A TiZr gasket, containing a powdered sample of silver(I) tricyanomethanide, fluorinert (a pressure transmitting medium) and a pellet of Pb (as pressure calibrant). Data were collected between

ambient pressure and 2 GPa, with data sets collected in the range $0 < d < 4.1$ Å. The calculated pressures were determined using a third-order Birch-Murnaghan Pb equation of state (V_0 = 30.354 Å^3, K_0 = 42.0 GPa and K' = 5.71).

3 Refinement Details

3.1 Single-Crystal X-ray Diffraction

Refinement details for variable-temperature single-crystal X-ray diffraction measurements are listed in Table S1, structural details for representative temperature points are given in Tables S2–S8, and full data collection and refinement details are given in the relevant crystallographic information files.

Structural refinement details for variable-pressure single-crystal measurements at ambient pressure and 0.83 GPa are given in Tables S9 and S10; full data collection and refinement details for these measurements are also provided in cif format.

Table S1: Crystallographic data collection details common to all variable-temperature and variable-pressure single-crystal X-ray diffraction measurements.

Radiation	Mo $K\alpha$, $\lambda = 0.71073$ Å
Formula	AgC_4N_3
M, g mol^{-1}	197.93
Z	4
Crystal Size (mm)	0.044 mm × 0.052 mm × 0.094 mm
Crystal System	Orthorhombic
Space Group	$Ima2$

Table S2: Single-crystal X-ray diffraction data collection and refinement details for Ag(*tcm*) at $T = 100$ K on heating.

a (Å)	8.0636(8)			
b (Å)	9.7766(9)			
c (Å)	6.2791(6)			
V (Å^3)	495.01(8)			
R ($I/\sigma > 2.0$)	0.0256			
Atom	x	y	z	U_{eq}, Å^2
Ag1	0.25	0.64736(5)	0.5546(2)	0.0176
N1	0.25	0.5139(8)	0.8313(11)	0.0257
C1	0.25	0.4525(9)	0.9888(12)	0.0162
N2	0.4718(6)	0.6835(5)	0.3470(7)	0.0191
C2	0.5973(7)	0.6570(6)	0.2735(8)	0.0145
C3	0.75	0.6219(9)	0.1798(12)	0.0156

Estimated standard errors are given in parentheses.

Table S3: Single-crystal X-ray diffraction data collection and refinement details for Ag(*tcm*) at $T = 150$ K on heating.

a (Å)	8.0513(5)			
b (Å)	9.8484(7)			
c (Å)	6.2666(4)			
V (Å^3)	496.89(6)			
R ($I/\sigma > 2.0$)	0.0229			
Atom	x	y	z	U_{eq}, Å^2
Ag1	0.25	0.64833(5)	0.5555(2)	0.0259
N1	0.25	0.5135(7)	0.8310(10)	0.0356
C1	0.25	0.4534(8)	0.9878(11)	0.0234
N2	0.4711(5)	0.6833(4)	0.3439(7)	0.0279
C2	0.5967(6)	0.6559(5)	0.2720(7)	0.0205
C3	0.75	0.6216(8)	0.1795(10)	0.0195

Estimated standard errors are given in parentheses.

Table S4: Single-crystal X-ray diffraction data collection and refinement details for Ag(*tcm*) at $T = 200$ K on heating.

a (Å)	8.0280(6)			
b (Å)	9.9637(10)			
c (Å)	6.2461(5)			
V (Å^3)	499.62(7)			
R ($I/\sigma > 2.0$)	0.0270			
Atom	x	y	z	U_{eq}, Å^2
Ag1	0.25	0.64942(6)	0.5569(3)	0.0355
N1	0.25	0.5137(9)	0.8300(12)	0.0451
C1	0.25	0.4531(10)	0.9854(13)	0.0297
N2	0.4709(7)	0.6832(5)	0.3420(9)	0.0375
C2	0.5970(8)	0.6562(6)	0.2696(9)	0.0277
C3	0.75	0.6199(9)	0.1765(12)	0.0267

Estimated standard errors are given in parentheses.

Table S5: Single-crystal X-ray diffraction data collection and refinement details for Ag(*tcm*) at $T = 250$ K on heating.

a (Å)	8.0075(6)			
b (Å)	10.0716(11)			
c (Å)	6.2278(5)			
V (Å^3)	502.26(8)			
R ($I/\sigma > 2.0$)	0.0319			
Atom	x	y	z	U_{eq}, Å^2
Ag1	0.25	0.65070(6)	0.5580(3)	0.0444
N1	0.25	0.5129(9)	0.8300(13)	0.0525
C1	0.25	0.4533(12)	0.9843(16)	0.0451
N2	0.4702(7)	0.6826(5)	0.3389(10)	0.0462
C2	0.5970(8)	0.6557(6)	0.2683(9)	0.0332
C3	0.75	0.6189(10)	0.1742(13)	0.0351

Estimated standard errors are given in parentheses.

Table S6: Single-crystal X-ray diffraction data collection and refinement details for Ag(*tcm*) at $T = 200$ K on cooling.

a (Å)	8.0260(6)			
b (Å)	9.9680(10)			
c (Å)	6.2459(4)			
V (Å^3)	499.69(7)			
R ($I/\sigma > 2.0$)	0.0300			
Atom	x	y	z	U_{eq}, Å^2
Ag1	0.25	0.64951(6)	0.5567(3)	0.0355
N1	0.25	0.5137(9)	0.8293(14)	0.0469
C1	0.25	0.4521(11)	0.9862(14)	0.0300
N2	0.4697(7)	0.6829(5)	0.3419(9)	0.0372
C2	0.5982(8)	0.6550(6)	0.2697(9)	0.0263
C3	0.75	0.6211(10)	0.1787(13)	0.0277

Estimated standard errors are given in parentheses.

Table S7: Single-crystal X-ray diffraction data collection and refinement details for Ag(*tcm*) at $T = 150$ K on cooling.

a (Å)	8.047(5)			
b (Å)	9.871(5)			
c (Å)	6.261(5)			
V (Å^3)	497.3(6)			
R ($I/\sigma > 2.0$)	0.0279			
Atom	x	y	z	U_{eq}, Å^2
Ag1	0.25	0.64836(5)	0.5559(2)	0.0259
N1	0.25	0.5146(7)	0.8302(10)	0.0344
C1	0.25	0.4523(9)	0.9877(11)	0.0204
N2	0.4712(6)	0.6838(5)	0.3450(7)	0.0279
C2	0.5975(6)	0.6563(5)	0.2707(8)	0.0200
C3	0.75	0.6208(8)	0.1779(10)	0.0167

Estimated standard errors are given in parentheses.

Table S8: Single-crystal X-ray diffraction data collection and refinement details for Ag(*tcm*) at $T = 100$ K on cooling.

a (Å)	8.0667(5)			
b (Å)	9.7791(6)			
c (Å)	6.2784(4)			
V (Å^3)	495.27(5)			
R ($I/\sigma > 2.0$)	0.0219			
Atom	x	y	z	U_{eq}, Å^2
Ag1	0.25	0.64735(4)	0.5547(2)	0.0172
N1	0.25	0.5144(7)	0.8319(10)	0.0249
C1	0.25	0.4534(8)	0.9888(10)	0.0155
N2	0.4715(5)	0.6830(4)	0.3459(6)	0.0190
C2	0.5977(6)	0.6562(5)	0.2736(7)	0.0153
C3	0.75	0.6208(7)	0.1795(10)	0.0138

Estimated standard errors are given in parentheses.

Table S9: Single-crystal X-ray diffraction data collection and refinement details for Ag(*tcm*) at $p = 0.08$ GPa.

a (Å)	7.9645(10)			
b (Å)	10.138(6)			
c (Å)	6.1945(10)			
V (Å^3)	500.2(3)			
R ($I/\sigma > 2.0$)	0.0451			
Atom	x	y	z	U_{eq}, Å^2
Ag1	0.25	0.6515(3)	0.5594(7)	0.0632
N1	0.25	0.514(4)	0.823(2)	0.050(3)
C1	0.25	0.459(4)	0.981(3)	0.048(3)
N2	0.4678(15)	0.6830(17)	0.3405(19)	0.050(2)
C2	0.5981(18)	0.652(3)	0.267(2)	0.048(2)
C3	0.75	0.615(3)	0.175(4)	0.048(2)

Estimated standard errors are given in parentheses.

Table S10: Single-crystal X-ray diffraction data collection and refinement details for Ag(*tcm*) at $p = 0.83$ GPa.

a (Å)	8.0121(13)			
b (Å)	9.646(6)			
c (Å)	6.2169(15)			
V (Å^3)	480.5(3)			
R ($I/\sigma > 2.0$)	0.0581			
Atom	x	y	z	U_{eq}, Å^2
Ag1	0.25	0.6517(4)	0.5559(10)	0.0557
N1	0.25	0.506(5)	0.828(4)	0.050(4)
C1	0.25	0.443(6)	0.987(4)	0.050(4)
N2	0.473(2)	0.684(2)	0.344(3)	0.050(4)
C2	0.600(2)	0.656(3)	0.272(3)	0.050(4)
C3	0.75	0.629(7)	0.180(5)	0.050(4)

Estimated standard errors are given in parentheses.

3.2 Powder Neutron Diffraction

A total of seven neutron powder diffraction patterns were collected at pressures within the stability field of ambient-phase Ag(*tcm*); these span the pressure range $0 < p < 0.615$ GPa. Unit cell dimensions were determined using the Pawley method and structures were subsequently refined using the Rietveld method, as implemented in Topas Academic.[S5] The line-shape function consisted of two back-to-back exponential functions convoluted with with a pseudo-voigt function. All atomic coordinates were freely refined. Distance restraints and angle restraints were applied to the *tcm*$^-$ ligands, with each C–C–N linkage restrained to be linear with bond lengths close to 1.156 Å. Atomic displacement parameters were modelled isotropically. Carbon and nitrogen atoms shared a common thermal parameter. The corresponding fits to data are shown in Fig. S1, and a summary of refined parameters is given in each of Tables S11–S17.

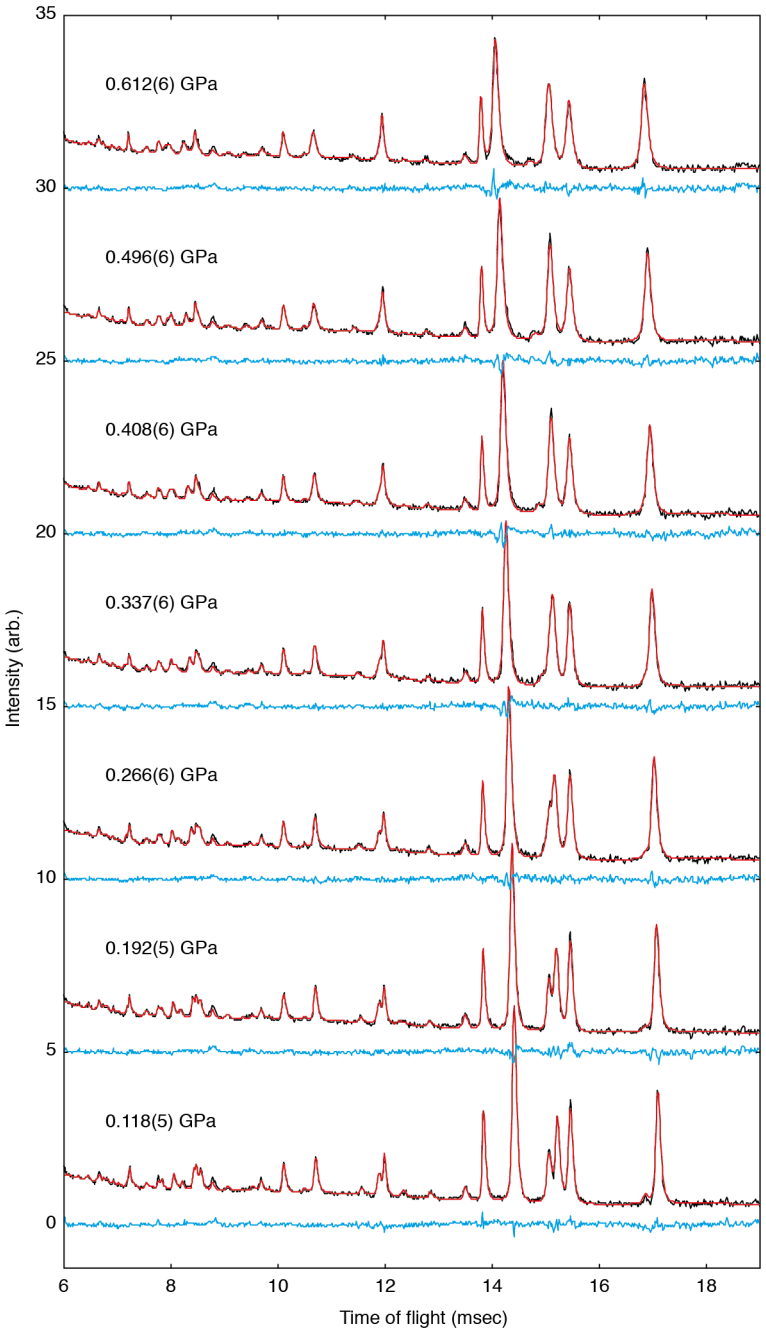

Figure S1: Powder neutron diffraction data (black lines), Rietveld fits (red lines) and difference curves (data − fit, blue curves). Data for successive pressure points have been translated by five intensity units.

Table S11: Neutron powder diffraction data refinement details for Ag(*tcm*) at $p = 0.118(5)$ GPa.

a (Å)	7.9913(6)			
b (Å)	10.1589(5)			
c (Å)	6.2122(5)			
V (Å^3)	504.33(6)			
R_{wp}	0.04139			
Atom	x	y	z	U_{iso}, Å^2
Ag1	0.25	0.651(2)	0.542(3)	0.0521(7)
N1	0.25	0.5123(3)	0.8173(8)	0.0309(17)
C1	0.25	0.44925(13)	0.9803(3)	0.0309(17)
N2	0.4649(6)	0.6842(2)	0.3332(4)	0.0309(17)
C2	0.5939(3)	0.65754(13)	0.2605(2)	0.0309(17)
C3	0.75	0.62515(19)	0.1727(4)	0.0309(17)

Estimated standard errors are given in parentheses.

Table S12: Neutron powder diffraction data refinement details for Ag(*tcm*) at $p = 0.190(5)$ GPa.

a (Å)	7.9910(6)			
b (Å)	10.1231(5)			
c (Å)	6.2142(5)			
V (Å^3)	502.69(6)			
R_{wp}	0.04078			
Atom	x	y	z	U_{iso}, Å^2
Ag1	0.25	0.648(2)	0.535(3)	0.046(6)
N1	0.25	0.5131(3)	0.8168(8)	0.039(2)
C1	0.25	0.44929(14)	0.9805(3)	0.039(2)
N2	0.4644(6)	0.6842(2)	0.3339(4)	0.039(2)
C2	0.5938(3)	0.65749(14)	0.2605(2)	0.039(2)
C3	0.75	0.6253(2)	0.1719(4)	4.3(4)

Estimated standard errors are given in parentheses.

Table S13: Neutron powder diffraction data refinement details for Ag(*tcm*) at $p = 0.265(6)$ GPa.

a (Å)	7.9924(7)			
b (Å)	10.0646(6)			
c (Å)	6.2175(6)			
V (Å^3)	500.13(7)			
R_{wp}	0.04126			
Atom	x	y	z	U_{iso}, Å^2
Ag1	0.25	0.646(2)	0.544(3)	0.047(7)
N1	0.25	0.5135(3)	0.8161(8)	0.037(2)
C1	0.25	0.44933(14)	0.9806(3)	0.037(2)
N2	0.4639(6)	0.6842(2)	0.3342(4)	0.037(2)
C2	0.5937(3)	0.65744(13)	0.2605(2)	0.037(2)
C3	0.75	0.6253(2)	0.1717(4)	4.0(4)

Estimated standard errors are given in parentheses.

Table S14: Neutron powder diffraction data refinement details for Ag(*tcm*) at $p = 0.336(6)$ GPa.

a (Å)	7.9931(7)			
b (Å)	10.0142(6)			
c (Å)	3.2207(7)			
V (Å^3)	497.93(8)			
R_{wp}	0.04109			
Atom	x	y	z	U_{iso}, Å^2
Ag1	0.25	0.652(2)	0.543(3)	0.060(8)
N1	0.25	0.5140(3)	0.8162(8)	0.032(2)
C1	0.25	0.44938(14)	0.9807(4)	0.032(2)
N2	0.4635(6)	0.6842(2)	0.3348(4)	0.032(2)
C2	0.5936(3)	0.65743(13)	0.2604(2)	0.032(2)
C3	0.75	0.6252(2)	0.1712(4)	4.1(4)

Estimated standard errors are given in parentheses.

Table S15: Neutron powder diffraction data refinement details for Ag(*tcm*) at $p = 0.409(6)$ GPa.

a (Å)	7.9930(10)			
b (Å)	9.9639(7)			
c (Å)	6.2228(10)			
V (Å^3)	495.59(10)			
R_{wp}	0.04092			
Atom	x	y	z	U_{iso}, Å^2
Ag1	0.25	0.651(2)	0.540(3)	0.055(7)
N1	0.25	0.5144(3)	0.8153(8)	0.035(2)
C1	0.25	0.44943(14)	0.9808(4)	0.035(2)
N2	0.4630(6)	0.6845(2)	0.3353(4)	0.035(2)
C2	0.5935(3)	0.65741(13)	0.2604(2)	0.035(2)
C3	0.75	0.6251(2)	0.1707(4)	0.035(2)

Estimated standard errors are given in parentheses.

Table S16: Neutron powder diffraction data refinement details for Ag(*tcm*) at $p = 0.500(6)$ GPa.

a (Å)	7.9990(11)			
b (Å)	9.9097(8)			
c (Å)	6.2218(12)			
V (Å^3)	493.19(12)			
R_{wp}	0.04243			
Atom	x	y	z	U_{iso}, Å^2
Ag1	0.25	0.646(2)	0.547(3)	0.046(7)
N1	0.25	0.5156(3)	0.8163(9)	0.029(2)
C1	0.25	0.44962(15)	0.9812(4)	0.029(2)
N2	0.4631(6)	0.6847(2)	0.3361(4)	0.029(2)
C2	0.5936(3)	0.65735(13)	0.2603(2)	0.029(2)
C3	0.75	0.6246(2)	0.1697(4)	0.029(2)

Estimated standard errors are given in parentheses.

Table S17: Neutron powder diffraction data refinement details for Ag(*tcm*) at $p = 0.615(6)$ GPa.

a (Å)	8.0013(10)			
b (Å)	9.8347(8)			
c (Å)	6.2239(11)			
V (Å^3)	489.77(11)			
R_{wp}	0.04119			
Atom	x	y	z	U_{iso}, Å^2
Ag1	0.25	0.648(2)	0.548(3)	0.034(6)
N1	0.25	0.5146(3)	0.8147(5)	0.036(2)
C1	0.25	0.44977(15)	0.9817(4)	0.036(2)
N2	0.4634(7)	0.6864(3)	0.3371(5)	0.036(2)
C2	0.5941(3)	0.65751(14)	0.2603(2)	0.036(2)
C3	0.75	0.6232(2)	0.1685(4)	0.036(2)

Estimated standard errors are given in parentheses.

3.3 High-Pressure Phase of Ag(*tcm*)

Profile fits to the high-pressure phase were possible using the Pawley method with a unit cell related to that of the orthorhombic, ambient phase. At a pressure of 0.672(7) GPa, we obtain a satisfactory fit — shown in Fig. S2 — using a primitive monoclinic cell. The loss of orthorhombic symmetry is evident in the splitting of some peaks (*e.g.* as highlighted by arrows within the inset graphic of the Figure) and in the statistically-significant deviation of the monoclinc cell angle β away from 90°. The loss of orthorhombic symmetry was supported by single-crystal X-ray data, collected at 1.47 and 2.39 GPa, although these data were of insufficient quality for structure determination. There is some indication from further peak splittings that the true symmetry of this high pressure phase may in fact be lower than monoclinic; however this distinction is difficult to make given the resolution and completeness of the data to hand. The monoclinic unit cell dimensions for the high pressure phase, as determined both by neutron powder and X-ray single-crystal diffraction, are given in Table S18.

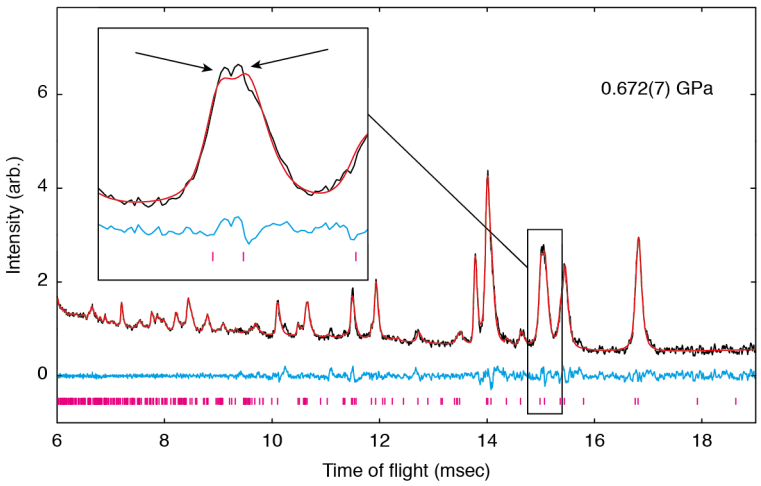

Figure S2: Pawley refinement of the neutron powder diffraction data for the high-pressure phase. Data are shown in black, the Pawley fit in red and the difference in blue. Reflections are represented by the pink tick marks. The inset graphic shows an expanded region of the pattern, indicated by the black box and the arrows show the peak splitting that is a consequence of symmetry lowering.

Table S18: Neutron powder diffraction data Pawley refinement and X-ray single-crystal unit cell determination for the high-pressure phase of Ag(*tcm*).

	Neutron powder	X-ray single-crystal	
p (GPa)	0.672(7)	1.47	2.39
a (Å)	7.9969(15)	8.028(4)	8.019(3)
b (Å)	9.7908(19)	9.290(18)	8.922(15)
c (Å)	6.2265(8)	6.193(3)	6.189(4)
β (°)	90.369(14)	90.30(6)	91.21(5)
V (Å^3)	487.50(14)	461.9(11)	442.7(8)

Estimated standard errors are given in parentheses.

4 Geometric derivations

4.1 Derivation of Inter-network Torsion Angle

A graphical representation of the relationship between the inter-network torsion angle θ and the Ag(*tcm*) crystal structure is given in Fig. S3. Straightforward trigonometric analysis gives:

$$\tan\left(\frac{\theta}{2}\right) = \frac{2(y_{\mathrm{N2}} - \frac{1}{2})b}{c}, \tag{1}$$

$$\theta = 2\tan^{-1}\left[\frac{2(y_{\mathrm{N2}} - \frac{1}{2})b}{c}\right]. \tag{2}$$

This is the expression used to determine the values of θ given in Tables S19–S21, and plotted in Fig. 2 of the main text. Uncertainties have been propagated in the usual way.

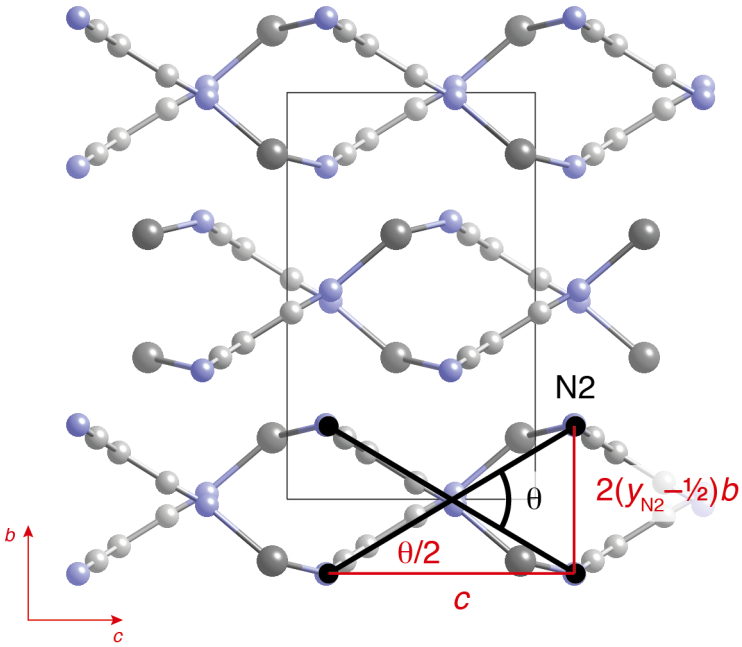

Figure S3: Geometric relationship used to determine the inter-network torsion angle θ. This representation of the crystal structure of Ag(*tcm*) is viewed down the **a** crystal axis. The four atoms covered by large black circles are all nitrogen N2 atoms.

4.2 Derivation of Equation (1)

The derivation of Eq. (1) of the main text makes use of the geometric relationship illustrated in Fig. S3. The length r is considered constant with respect to temperature and/or pressure (*i.e.* the bond lengths within the honeycomb lattice of Ag(*tcm*) are considered temperature-/pressure-independent). We then have

$$\ell = r\cos\left(\frac{\theta}{2}\right), \tag{3}$$

$$\frac{\mathrm{d}\ell}{\mathrm{d}T} = -r\sin\left(\frac{\theta}{2}\right)\cdot\frac{1}{2}\frac{\mathrm{d}\theta}{\mathrm{d}T}. \tag{4}$$

Hence

$$\alpha_A = \frac{2}{\ell}\frac{\mathrm{d}\ell}{\mathrm{d}T} = -\frac{r\sin\left(\frac{\theta}{2}\right)}{r\cos\left(\frac{\theta}{2}\right)}\cdot\frac{\mathrm{d}\theta}{\mathrm{d}T} \tag{5}$$

$$= -\theta\tan\left(\frac{\theta}{2}\right)\alpha_\theta, \tag{6}$$

as required. The analogous expression

$$K_A = -\theta\tan\left(\frac{\theta}{2}\right)K_\theta \tag{7}$$

can be derived using the same approach.

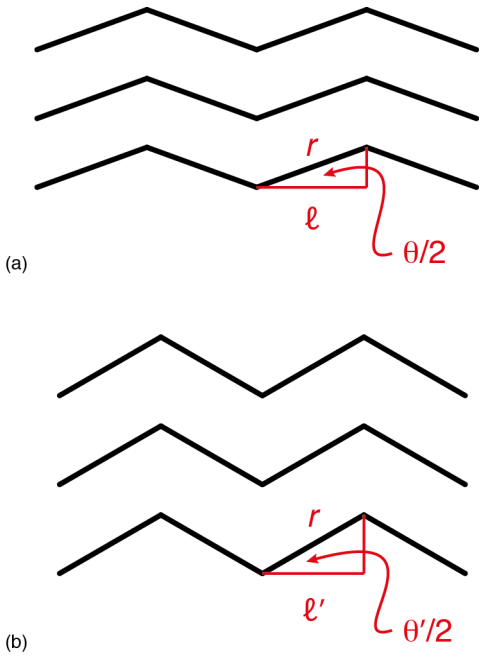

Figure S4: Geometric relationship used to derive Eq. (1) in the main text. This is a schematic representation of a puckered, layered, system in two states (*e.g.*, temperatures or pressures) (a) and (b). The total layer area, which is proportional to r^2, is conserved in both states; the deformation mechanism involves a change in the puckering angle $\theta/2$ (the factor of two included for consistence with the derivation in section S4.1). The corresponding change in cross-sectional length ℓ can be used to relate the rate of change of θ to a corresponding area coefficient of thermal expansion α_A or area compressibility K_A.

5 Lattice Parameter and Inter-Network Torsion Angle Variation

5.1 Single-Crystal X-ray Diffraction

Lattice parameter values, y_{N2} values, and derived θ values obtained from structural refinements against variable-temperature single-crystal X-ray diffraction data are given in Tables S19 and S20 (warming and cooling runs, respectively). The data at two temperatures (160 and 170 K) in the warming cycle were not of sufficient quality to obtain reliable positional parameters, so only lattice parameters are reported for these temperatures.

Table S19: Variable-temperature structural parameter data as determined on warming using single-crystal X-ray diffraction.

T (K)	a (Å)	b (Å)	c (Å)	y_{N2}	θ (°)
100	8.0636(8)	9.7766(9)	6.2791(6)	0.6835(5)	59.49(13)
110	8.0597(6)	9.7942(7)	6.2760(4)	0.6845(4)	59.87(11)
120	8.0580(5)	9.8108(7)	6.2729(4)	0.6835(4)	59.71(11)
130	8.0556(5)	9.8297(7)	6.2697(4)	0.6838(5)	59.91(13)
140	8.0513(5)	9.8484(7)	6.2666(4)	0.6843(5)	60.17(13)
150	8.0584(6)	9.8752(8)	6.2692(5)	0.6833(4)	60.01(11)
160	8.0564(6)	9.8969(9)	6.2670(5)	0.6835(4)	60.19(11)
170	8.0523(6)	9.9156(9)	6.2625(5)	0.6830(4)	60.18(11)
190	8.0297(5)	9.9450(9)	6.2504(4)	0.6840(5)	60.70(14)
200	8.0280(6)	9.9637(10)	6.2461(5)	0.6832(5)	60.61(14)
210	8.0226(6)	9.9881(10)	6.2426(5)	0.6824(5)	60.54(14)
220	8.0197(6)	10.0080(11)	6.2384(5)	0.6825(5)	60.70(14)
230	8.0149(6)	10.0302(11)	6.2344(4)	0.6826(5)	60.87(14)
240	8.0109(6)	10.0514(11)	6.2310(4)	0.6825(5)	60.98(14)
250	8.0075(6)	10.0716(11)	6.2278(4)	0.6826(5)	61.13(14)

Estimated standard errors are given in parentheses.

Table S20: Variable-temperature structural parameter data as determined on cooling using single-crystal X-ray diffraction.

T (K)	a (Å)	b (Å)	c (Å)	y_{N2}	θ (°)
240	8.0119(6)	10.0501(11)	6.2301(4)	0.6828(6)	61.06(16)
230	8.0148(6)	10.0301(10)	6.2349(4)	0.6828(6)	60.92(16)
220	8.0189(6)	10.0092(11)	6.2378(5)	0.6824(5)	60.69(14)
210	8.0224(6)	9.9884(10)	6.2417(4)	0.6828(5)	60.66(14)
200	8.0260(6)	9.9680(10)	6.2459(4)	0.6829(5)	60.55(14)
190	8.0318(6)	9.9472(9)	6.2491(4)	0.6833(5)	60.53(14)
180	8.0359(5)	9.9261(8)	6.2525(4)	0.6829(5)	60.29(14)
170	8.0389(6)	9.9083(8)	6.2553(4)	0.6839(5)	60.45(14)
160	8.0428(6)	9.8892(8)	6.2586(4)	0.6838(5)	60.30(14)
150	8.0469(6)	9.8711(8)	6.2615(4)	0.6838(5)	60.19(14)
140	8.0492(5)	9.8524(7)	6.2644(4)	0.6837(5)	60.04(14)
130	8.0526(5)	9.8334(7)	6.2677(4)	0.6835(4)	59.87(11)
120	8.0572(5)	9.8159(7)	6.2707(4)	0.6844(4)	60.00(11)
110	8.0621(5)	9.7970(7)	6.2755(4)	0.6832(4)	59.54(11)
100	8.0667(5)	9.7791(6)	6.2784(4)	0.6835(5)	59.51(140

Estimated standard errors are given in parentheses.

5.2 Powder Neutron Diffraction

Lattice parameter values, y_{N2} values, and derived θ values obtained from structural refinements against variable-pressure powder neutron diffraction data are given in Table S21.

Table S21: Variable-pressure structural parameter data as determined using powder neutron diffraction.

p (GPa)	a (Å)	b (Å)	c (Å)	y_{N2}	θ (°)
0.118(5)	7.9913(6)	10.1589(5)	6.2122(5)	0.6842(2)	62.14(6)
0.190(5)	7.9910(6)	10.1231(5)	6.2142(5)	0.6842(2)	61.92(6)
0.265(6)	7.9924(7)	10.0646(6)	6.2175(5)	0.6842(2)	61.63(6)
0.336(6)	7.9931(7)	10.0142(6)	6.2207(7)	0.6842(2)	61.34(6)
0.409(6)	7.9930(10)	9.9639(7)	6.2228(10)	0.6845(2)	61.16(6)
0.500(6)	7.9990(11)	9.9097(8)	6.2218(11)	0.6847(2)	60.95(7)
0.615(6)	8.0013(10)	9.8347(5)	6.2239(11)	0.6864(3)	61.01(7)

Estimated standard errors are given in parentheses.

6 References

(S1) J. Cosier, A. Glazer, *J. Appl. Cryst.* **19**, 105 (1986).
(S2) A. Altomare, *et al.*, *J. Appl. Cryst.* **27** (1994).
(S3) P. Betteridge, J. Carruthers, R. Cooper, K. Prout, D. Watkin, *J. Appl. Cryst.* **36** (2003).
(S4) G. J. Piermarini, S. Block, J. D. Barnett, R. A. Forman, *J. Appl. Phys.* **46**, 2774 (1975).
(S5) A. Coelho, Topas-academic: General profile and structural analysis software for powder diffraction data. version 4.1., *Tech. rep.*, Brisbane, Australia (2007).